6.541 24.968 HST 701 Handout 1

5 Feb 10

Table 5.1 List of articulator-free features and their values for different classes of segments

Feature	Vowels	Glides	Consonants	n,l	t,b	s,z	θ,ð
Vocalic	+	−	−	−	−	−	−
Consonantal	−	−	+	+	+	+	+
Continuant				−	−	+	+
Sonorant				+	−	−	−
Strident						+	−

Note: The segment labels at the top of the last four columns are examples of the segments with the given feature values.

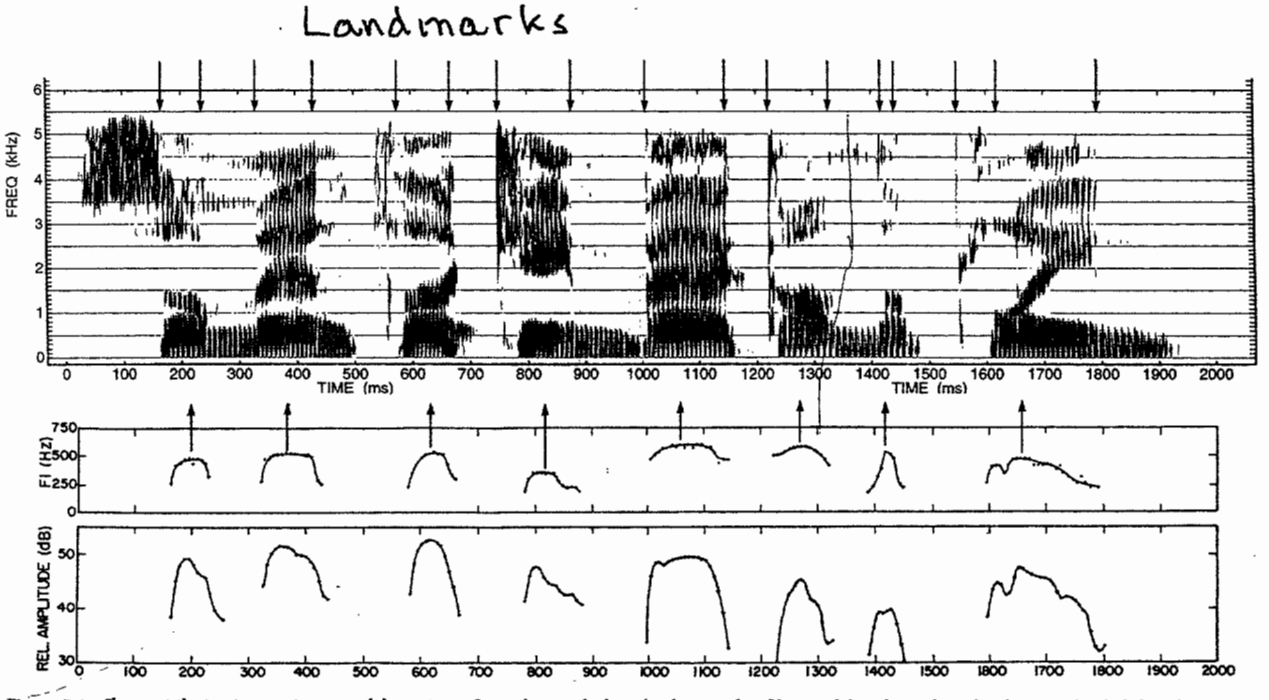

Figure 5.1 Shown at the top is a spectrogram of the sentence *Samantha came back on the plane*, produced by an adult male speaker. The plot immediately below the spectrogram gives the frequency of *F1* vs. time during the vocalic regions, measured at 7.5-ms intervals. At the bottom is a plot of the relative amplitude of the first-formant prominence during the vocalic regions. Each point on this amplitude plot and on the plot of frequency of *F1* is measured from a spectrum which is obtained by averaging a 10-ms sequence of spectra, each of which is calculated using a 6.4-ms Hamming window. The arrows below the spectrogram indicate vocalic landmarks and the arrows at the top identify consonantal landmarks. See text.

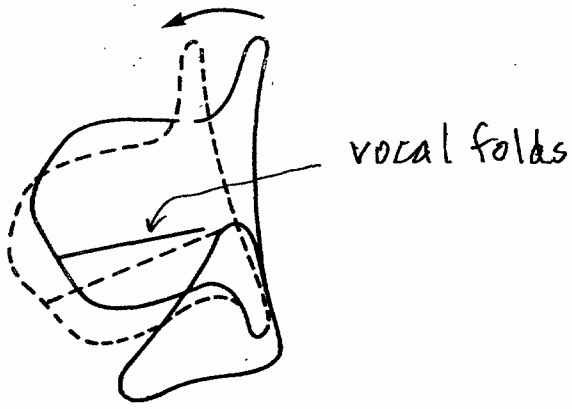

Figure 1.7 Midsagittal view showing the rocking motion of the thyroid cartilage in relation to the cricoid cartilage. The vocal folds are schematized by the solid and dashed straight lines.

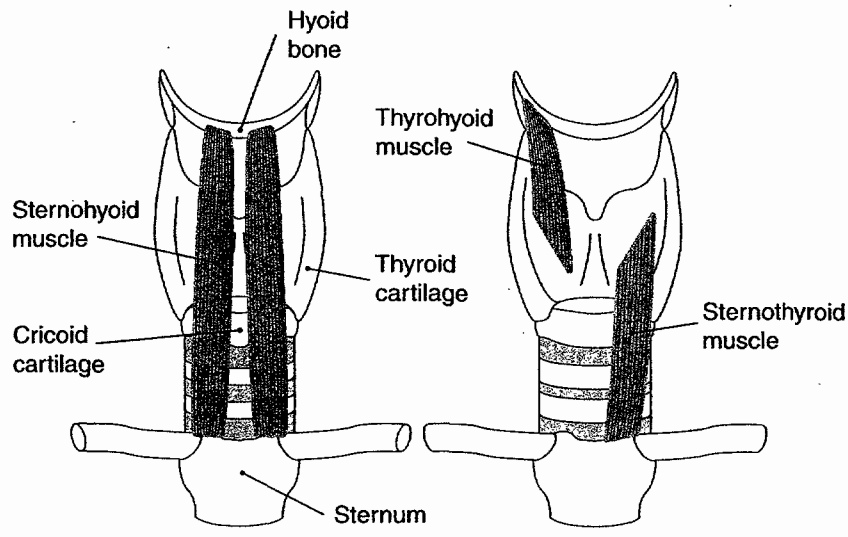

Figure 1.12 Schematic representations of the sternohyoid muscles (left) and the thyrohyoid and sternothyroid muscles (right).

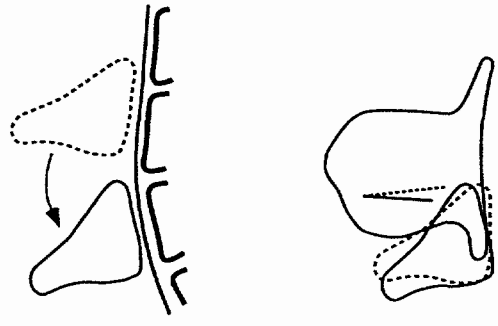

Figure 1.13 The drawing on the left shows how the cricoid cartilage can tilt forward as the larynx is lowered through the action of the sternohyoid and sternothyroid muscles. The drawing on the right illustrates how this tilting can rotate the cricoid cartilage relative to the thyroid cartilage, thereby shortening the vocal folds and decreasing their stiffness. (After Honda et al., 1993.)

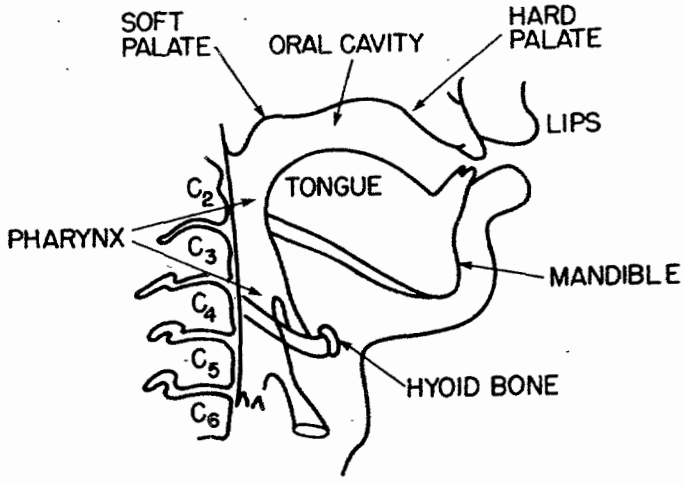

Figure 1.14 Midsagittal section of the vocal tract and surrounding structures, as obtained by tracing from a radiograph. The wings of the mandible and hyoid bone and the tips of the arytenoid cartilages are shown, although they are not in the midsagittal plane. The cervical vertebrae C1–6 are identified. (From Perkell, 1969.)

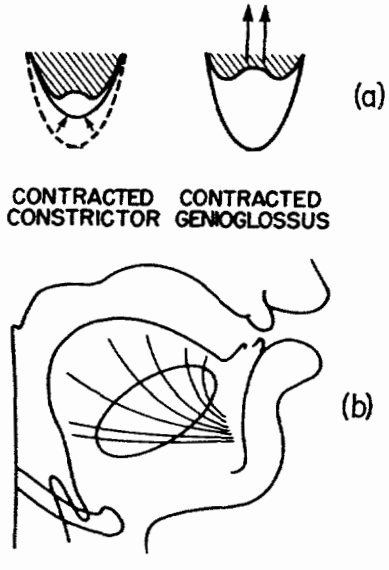

Figure 1.15 Illustrating how the constrictor muscles and the lower fibers of the genioglossus muscle operate to change the shape of the airway in the pharyngeal region. (a) Schematic representation of the airway shape when the pharynx is narrowed (left) by the contraction of a constrictor muscle (the dashed line indicating the configuration in the absence of muscle contraction), and when the pharynx is widened (right) by contraction of the genioglossus muscle. (b) A sketch of the fibers of the genioglossus muscle in the lateral view.

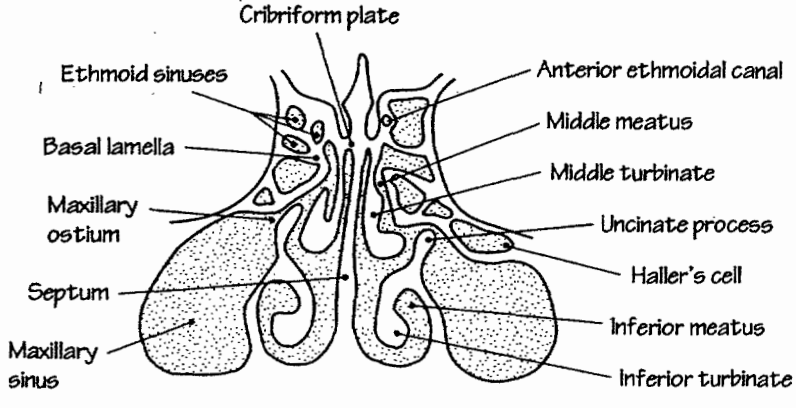

Figure 1.18 This coronal view of the nasal cavity was taken at about the middle of the nasal cavity so that some of the sinuses and undulations are not shown. The middle and inferior turbinates and the paranasal sinuses increase the total surface area of the nasal cavity. (Revised figure from Rice and Schaefer, 1993.)

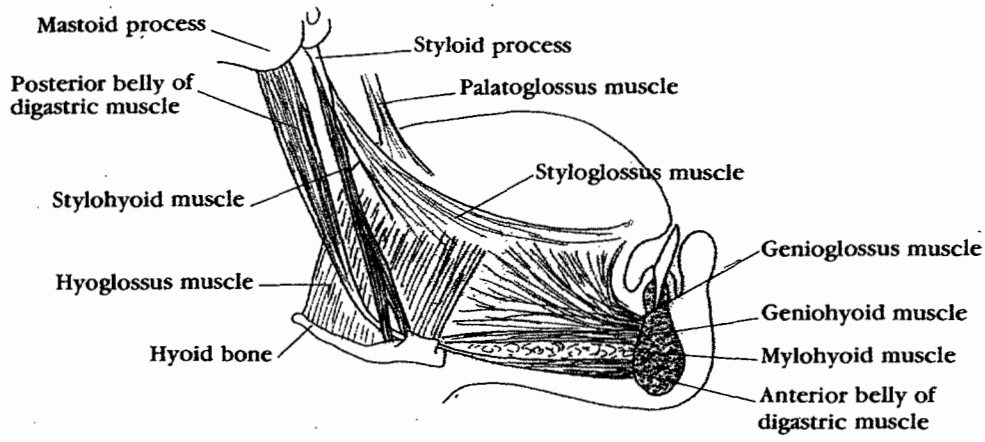

Figure 1.21 Extrinsic muscles of the tongue as viewed in lateral dissection. (From Dickson and Maue-Dickson, 1982.)

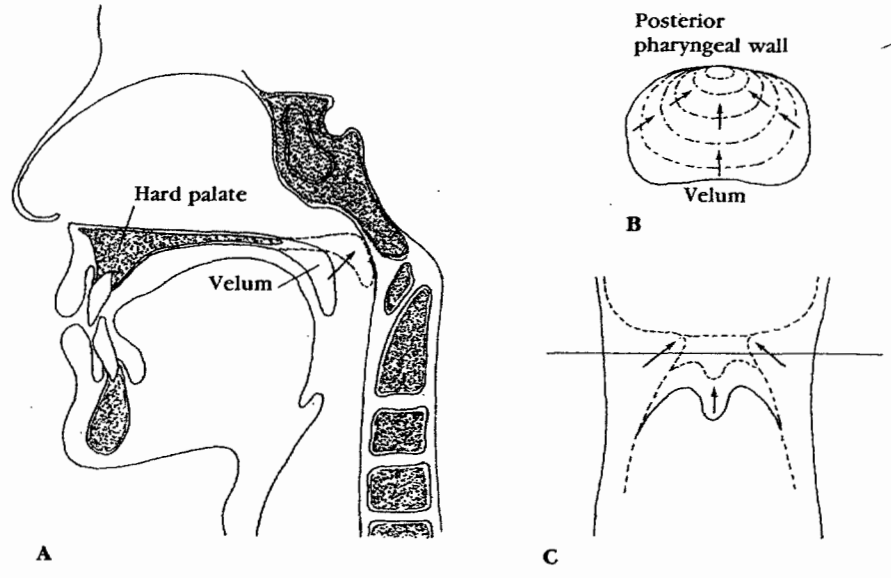

Figure 1.17 Showing how velopharyngeal closure is achieved. Solid lines represent the open position and dashed lines with arrows represent various positions toward closure. (a) Lateral view; (b) superior view; (c) anterior view. The figure shows that the closing maneuver involves raising of the velum in conjunction with an inward movement of the pharyngeal walls. (From Dickson and Maue-Dickson, 1982.)

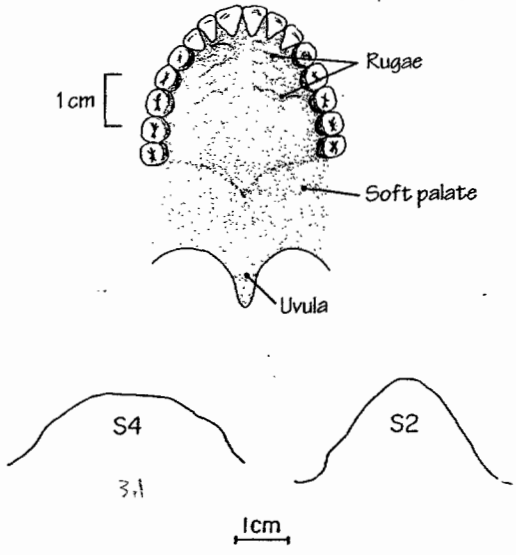

Figure 1.20 (a) Sketch of surfaces of hard and soft palate, showing arrangement of teeth around the palate. (From Dickson and Maue-Dickson, 1982.) The scale at the left is estimated. (b) Coronal section of hard palate in the vicinity of the molars for two adult males, showing individual differences in the vertical depth of the palate. (From Perkell et al., 1995.)